JACS
JOURNAL OF THE AMERICAN CHEMICAL SOCIETY
Article
pubs.acs.org/JACS

A New Strategy for Intracellular Delivery of Enzyme Using Mesoporous Silica Nanoparticles: Superoxide Dismutase

Yi-Ping Chen,[†] Chien-Tsu Chen,[‡] Yann Hung,[†] Chih-Ming Chou,[‡] Tsang-Pai Liu,[§,∥] Ming-Ren Liang,[†] Chao-Tsen Chen,[†] and Chung-Yuan Mou*[,†]

[†]Department of Chemistry, National Taiwan University, Taipei 106, Taiwan
[‡]Department of Biochemistry, Taipei Medical University, Taipei 106, Taiwan
[§]Division of General Surgery, Department of Surgery, Mackay Memorial Hospital, Taipei 106, Taiwan
[∥]Mackay Medicine, Nursing and Management College, Taipei 106, Taiwan

Supporting Information

ABSTRACT: We developed mesoporous silica nanoparticle (MSN) as a multifunctional vehicle for enzyme delivery. Enhanced transmembrane delivery of a superoxide dismutase (SOD) enzyme embedded in MSN was demonstrated. Conjugation of the cell-penetrating peptide derived from the human immunodeficiency virus 1 (HIV) transactivator protein (TAT) to mesoporous silica nanoparticle is shown to be an effective way to enhance transmembrane delivery of nanoparticles for intracellular and molecular therapy. Cu,Zn-superoxide dismutase (SOD) is a key antioxidant enzyme that detoxifies intracellular reactive oxygen species, ROS, thereby protecting cells from oxidative damage. In this study, we fused a human Cu,Zn-SOD gene with TAT in a bacterial expression vector to produce a genetic in-frame His-tagged TAT-SOD fusion protein. The His-tagged TAT-SOD fusion protein was expressed in *E. coli* using IPTG induction and purified using FMSN-Ni-NTA. The purified TAT-SOD was conjugated to FITC-MSN forming FMSN-TAT-SOD. The effectiveness of FMSN-TAT-SOD as an agent against ROS was investigated, which included the level of ROS and apoptosis after free radicals induction and functional recovery after ROS damage. Confocal microscopy on live unfixed cells and flow cytometry analysis showed characteristic nonendosomal distribution of FMSN-TAT-SOD. Results suggested that FMSN-TAT-SOD may provide a strategy for the therapeutic delivery of antioxidant enzymes that protect cells from ROS damage.

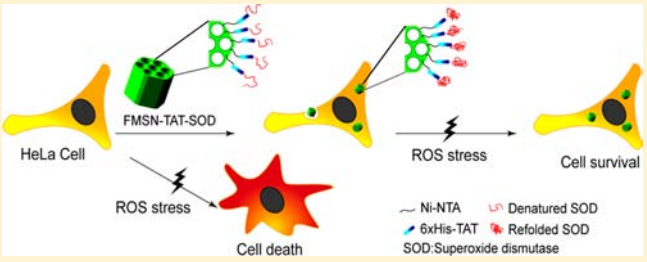

INTRODUCTION

Intracellular protein delivery is receiving increasing attention for treatment of protein deficiency, mutation, and misfolding diseases such as amyotrophic lateral sclerosis (ALS) and Parkinson's Disease.[1−3] To restore biological function of proteins relevant to protein abnormal diseases, protein-based therapy has been developed.[4] The idea is to repair the protein-mediated diseases through the delivery of normal protein in vitro or in vivo. Some strategies have been used to manipulate cell functions by influencing signaling pathways.[5,6] For example, we can regulate the biomarkers of p53 and caspase to turn on/off the cell death for the diseases of apoptosis pathways. Delivering antigens to a specific site to stimulate a desired immune response has been explored.[7] Protein therapy offers a new direction for the next generation of medicine.

However, applications of protein-based therapies remain rare, partly due to the intrinsic properties of most proteins: poor stability and membrane permeability. In addition, endosome trapping and digestion, which often occur during intracellular protein delivery, significantly limit the treatment efficiency. In recent years, there have been two main strategies for overcoming these problems: (a) nanoparticles (NPs) as a carrier for delivery of protein; engineered multifunctional nanoparticles with targeting specific cells, cell-tracking signal, and cargo-delivery capacity have been extensively developed, and its extension to carry protein as cargo would certainly be very interesting; and (b) fusogenic peptides (TAT) to increase cell uptake and avoid endosome trapping; the human immunodeficiency virus 1 (HIV) TAT peptide containing a small region of residues YGRKKRRQRRR (TAT peptide) had been reported as one of the most effective carrier peptides, which has been proven to effectively translocate proteins across cell membrane in an apparently energy-independent manner. The TAT peptide is able to mediate nanoparticles across the blood−brain barrier (BBB) and locate them around the cell nucleus of neurons.[8]

Our strategy is to combine a nanoparticle carrier and TAT fusogenic peptide by surface functionalization of nanoparticle and recombinant gene expression of protein (enzyme). Mesoporous silica nanoparticle (MSN) is one of the promising nanoparticles to serve as a multifunctional vehicle due to its

Received: October 30, 2012
Published: January 5, 2013

   dx.doi.org/10.1021/ja3105208 | J. Am. Chem. Soc. 2013, 135, 1516−1523

high surface area, uniform pore size, easy functionalization, and biocompatibility. Therefore, it becomes highly suitable for biological applications.[9−12] Here, we demonstrate the conjugated complex with a nonpermeable antioxidant enzyme, Cu,Zn-superoxide dismutase (SOD), will cross the cell membrane efficiently. MSNs (with diameters between 50 and 100 nm) readily undergo an endocytosis in vitro with much higher cellular uptake efficiency than the passive transfer or simple diffusion of molecules across cell membranes.[13] We prepared the TAT-SOD fusion protein by a recombinant DNA technique with built-in 6xHis codes to produce His-tag protein. The TAT-SOD was expressed in *E. coli* using IPTG induction and purified using FMSN-Ni-NTA by a one-step metal affinity binding. Herein, we demonstrate a simple method for preparation in aqueous solution of His-tag protein without using organic solvents. In addition, the interactions by metal affinity between TAT-SOD proteins and MSN nanoparticles afford an advantage to isolate the His-tag TAT-SOD from the whole cell lysate without any further purification step. At the same time, the successful interactions of FMSN-Ni-NTA and His-tag TAT-SOD enable the conjugate complex, which can be selectively isolated as sediment, to be directly formed.

In addition to traditional applications of mesoporous silica such as catalysis[14] and chromatography,[15] biomedical applications of MSN such as enzyme immobilization,[16] gene transfection,[17,18] and drug delivery agents[19] have recently gained much attention.[20,21] We previously reported that MSNs function in cell labeling[13,22] and stem cell tracking.[23] In this work, a new method of conjugating protein to the surface of MSN for delivery has been designed. We choose to study the enzyme, Cu,Zn-superoxide dismutase (SOD),[24] which is a key antioxidant enzyme that detoxifies intracellular reactive oxygen species (ROS), thereby protecting cells from oxidative damage.

Reactive oxygen species (ROS), such as free radicals and peroxides, lead to oxidative damage in cells or tissue. There are many different endogenous and exogenous sources by which the reactive oxygen species are generated. The level of oxidative stress is determined by the balance between the rate at which oxidative damage is induced and the rate at which it is efficiently repaired and removed. Antioxidant enzymes, such as superoxide dismutase, have been found to exert a beneficial effect against various diseases that are mediated by the reactive oxygen species.

In this study, a recombinant gene of human Cu,Zn-superoxide dismutase (hSOD) fused with human immunodeficiency virus 1 (HIV) transducing peptide (TAT) was constructed in a bacterial expression vector to overproduce a genetic in-frame TAT-SOD fusion protein. The TAT-SOD was conjugated to FMSN with a tether in a nickel-oligo histidine interaction forming FMSN-TAT-SOD. The biological characterization of FMSN-TAT-SOD as an agent against ROS was investigated, which included the level of ROS and apoptosis after free radicals induction, functional recovery after ROS damage, and activation of caspase-9 and p21 in culture cells. We will show that FMSN-TAT-SOD may provide a useful strategy for the therapeutic delivery of antioxidant enzymes that protect cells from ROS damage.

RESULTS AND DISCUSSION

Previously, we have reported the synthesis of size-controlled multifunctional mesoporous silica nanoparticle (MSN) and found that MSN of 50 nm gives the highest cell-uptake.[25] For the purpose of tracking the uptaken MSN in the cells, we thus chose the 50 nm diameter MSN with functionalization of a fluorescent organic dye, fluorescein isothiocyanate (FITC), to form FITC-MSN (FMSN). For further conjugation of protein to the MSN surface, we introduced Ni-NTA surface functionality to interact with the His-tagged protein. We modified the FMSN surface with a nitrilotriacetic acid tether, NTA silane, which thereafter reacted with nickel metal ion (Scheme 1).

Scheme 1. Schematic Illustration for the Ni-NTA-Modified FMSN That Interacts Selectively with Histidine-Tagged TAT-SOD Protein and Subsequently Gives a Protective Effect on Cells against Oxidative Stress[a]

[a](a) First, we modified the FMSN with Ni-NTA to form FMSN-Ni-NTA. Next, 6xHis-TAT-SOD was cloned and overexpressed by *E. coli* using molecular biology method. The FMSN-Ni-NTA selectively bound to histidine-tagged TAT-SOD protein in an *E. coli* cell lysate. 8 M urea was used to denature the TAT-SOD protein. (b) After the cell delivery, the denatured TAT-SOD protein could be refolded to catalyze with full activity.

For the subsequent experiment of FMSN-SOD conjugation, we overexpressed and purified the His-tag human Cu,Zn-superoxide dismutase (SOD) protein containing a human immunodeficiency virus 1 (HIV) transducing domain (Tat 49−57; TAT) from a human TAT-SOD gene in-frame constructed in pQE-30 vector (pQE-TAT-SOD) as described in Chou et al. (2005) (Figure 1a).[26] The construct was transformed into JM109 *E. coli* cells and cultured in LB broth with IPTG induction. The harvested bacterial cells were lysed at 4 °C in a 10% glycerol/ddH_2O buffer. Protein content in the crude cell extract (supernatant) obtained from the lysate was determined, and then the overexpression of TAT-SOD was confirmed with electrophoresis in 12% SDS-PAGE. The protein bands were visualized by staining with Coomassie brilliant blue G250 showing a major 23 kD band (Figure 1b). The band marked by an arrow in lane 2 (1 h), lane 3 (2 h), and lane 4 (3 h), in comparison with that of the lane 1 (0 h), suggested that the SOD protein was expressed at increasingly higher level with increasing induction time. A major problem for efficient delivery of a MSN-mediated agent into the cytoplasm of living

dx.doi.org/10.1021/ja3105208 | J. Am. Chem. Soc. 2013, 135, 1516−1523

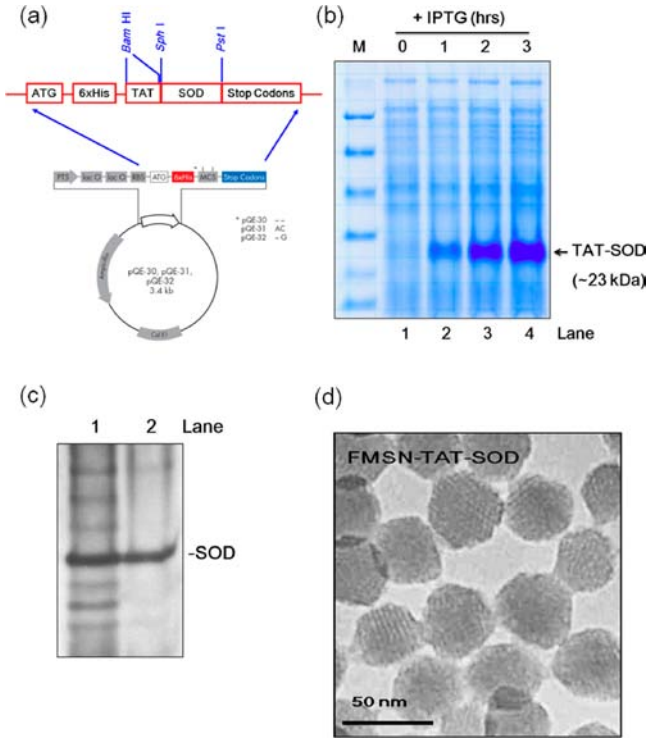

Figure 1. Bioconjugation of TAT-SOD with MSN nanoparticles. (a) Construct of the pQE-TAT-SOD. The synthetic TAT oligomer was cloned into the *Bam* HI site, and human Cu,Zn SOD cDNA was cloned into *Sph* I and *Pst* I sites of vector pQE. (b) Electrophoretic analysis of IPTG induced overexpression of Human Cu,Zn-SOD protein. The SOD protein was induced and overexpressed from pQE-TAT-SOD within 1, 2, and 3 h by IPTG in *E. coli* and analyzed by electrophoresis in a 12% SDS-PAGE. (c) Western blotting analysis of the purified SOD. The FMSN-Ni-NTA purified SOD shown as lane 2 as compared to *E. coli* total lysate (lane 1) by using Western blot analysis with a polyclonal antibody to human SOD. (d) TEM image of FMSN-TAT-SOD. The average diameter of MSN is 50 nm.

cells is that the nanoparticles may often be trapped in organelles such as endosomes and lysosomes. Previously, it has been reported that TAT-mediated delivery would result in a nonendosomal mechanism for cell-uptake.[27] The design of FMSN-TAT-SOD was to avoid the endosomal trap inside living cells.

The second important consideration in design is to ensure a binding of protein to the external surface of nanoparticles (NPs), which is convenient and specific. In this work, we take advantage of the affinity interactions[28,29] between Ni-NTA-bearing MSN with His-tagged proteins. The affinity between Ni-NTA and oligohistidine ($K_d \approx 10^{-13}$) has been shown to be comparable to or superior than that of the protein−protein interaction ($K_d \approx 10^{-5}$−10^{-12}) such as carbohydrate−lectin or streptavidin−biotin interactions.[30−32] Therefore, the use of such an interaction can provide a simple and sensitive method that would overcome the limitation of conventional antibody-based protein labeling. Particularly, we designed a novel one-step method achieving the isolation and conjugation at the same time. The design is based on the interaction between Ni-NTA-NPs and His-tagged proteins.[33] In the nickel bead purification procedure, the His-tag TAT-SOD proteins are associated with Ni(II) to form Nickel-6xHis complex, and the metal affinity could be dissociated by adding excessive imidazole. For one-step isolation and conjugation, the immobilized TAT-SOD via formation of Nickel-6xHis interaction on the FMSN surface was isolated by centrifugation at 7000 rpm for 20 min and subsequently purified by removing the supernatant. This procedure affords an easy and clean separation of the FMSN-TAT-SOD protein conjugates. The Western blotting assay was used to identify the SOD molecule by a polyclonal antibody against human SOD and confirm the protein associated with FMSN. Results (Figure 1c) indicated that the SOD protein dissociated from FMSN by the imidazole elution was clean, and the immunological recognition suggested the SOD protein attached to FMSN through metal affinity interaction. This conjugated complex has the following advantages: (a) high affinity resulting in quantitative binding and stability, (b) specificity for His-tag engineered proteins, and (c) reversible binding, which could be dissociated by imidazole. After the one-step purification, the TAT-SOD molecule was denatured by treating FMSN-TAT-SOD with 8 M urea. Here, we would like to mention that the SOD in as-synthesized FMSN-TAT-SOD, FMSN-SOD, and TAT-SOD were all in denatured form for subsequent experiments.

To further investigate the amount of TAT-SOD and Ni attached on the MSN, the Bradford method and ICP-MS elemental analysis were used, respectively. The amount of SOD protein attached on FMSN was determined by measuring the SOD molecules dissociated in the supernatant through the imidazole buffer elution. We determined an average weight percent of TAT-SOD in FMSN-TAT-SOD at 16.7 wt % and Ni at 0.3 wt %. Thus, the Ni to SOD ratio is about 7:1. The transmission electron microscopic (TEM) image in Figure 1d shows the FMSN-TAT-SOD possesses an average diameter of 50 nm and well-ordered mesopores. The zeta potential is in the range from −30 to −35 mV. The surface functionalizations of TAT, NTA, and SOD had very little influence on the total charge of the FMSN (see Figure S5).

We then proceed to evaluate the delivery efficiency of FMSN-TAT-SOD into cells in vitro. FMSN-TAT-SOD was added to the culture media of HeLa cells and incubated for 4 h. Harvested cells were lysed and treated with 500 mM imidazole. Western blotting of cell lysate was carried out to analyze the content of cellular SOD (Figure 2a). The control cells without any external loading of SOD show a weak presence of intrinsic SOD. In comparison, cells with treatments of FMSN-TAT-SOD give a very strong SOD signal, which indicated the TAT-SOD protein has been transduced into the HeLa cells. To determine the cellular localization of the transduced TAT-SOD proteins, FMSN-TAT-SOD treated HeLa cells were fixed for the immuno-cytostaining with DNA-specific DAPI (blue) and anti-SOD antibody (red). Confocal microscopy observations (Figure 2b) show colocalization image (yellow) of FMSN (green) and SOD protein (red) in the FMSN-TAT-SOD-delivered cells, whereas the cells with FMSN alone show only green signal from the FITC fluorescence. In the cells treated with FMSN only (upper row of Figure 2b), the fluorescence signal of endogenous SOD protein was apparently low.

The restoration of enzymatic activities of TAT-SOD protein in cells is critical for the application of protein transduction for therapeutic use. In our strategy, the denatured form of SOD would be refolded back into the native form of SOD, which is regulated by intracellular chaperons[34] such as Hsp90.[35] Therefore, we examined the SOD activities in the HeLa cells, which had been delivered with denatured FMSN-TAT-SOD proteins as mentioned before (Figure 2c). Here, we show that denatured FMSN-TAT-SOD could successfully enter the HeLa

dx.doi.org/10.1021/ja3105208 | J. Am. Chem. Soc. 2013, 135, 1516−1523

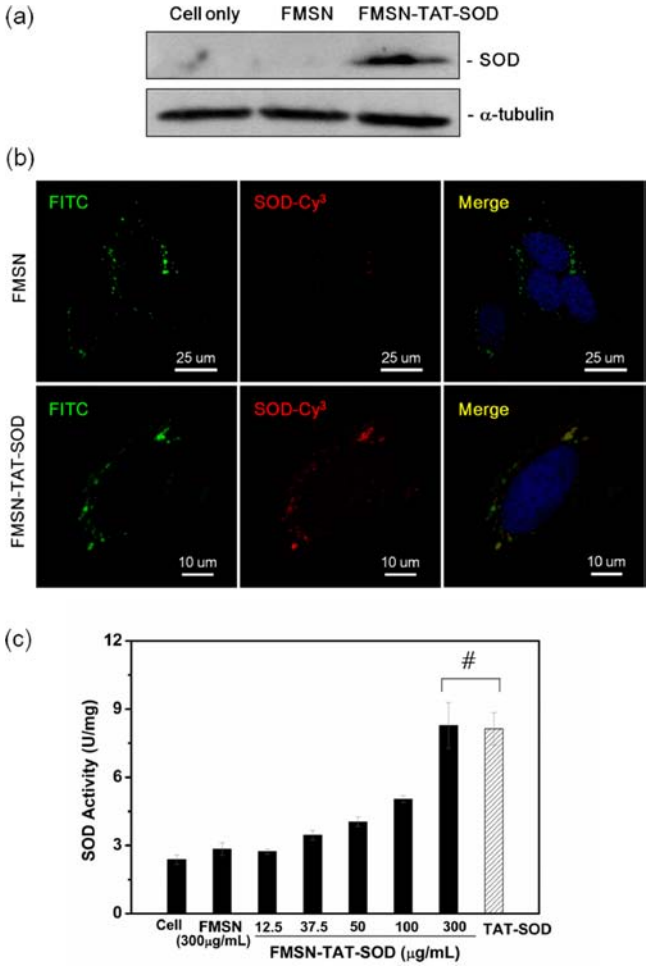

Figure 2. Delivery of FMSN-TAT-SOD into HeLa cells. FMSN-TAT-SOD and bare FMSN were added to the serum free cultured media for 4 h. (a) Cellular delivery of SOD by FMSN-TAT-SOD. The cells were sonicated with lysis buffer containing 500 mM imidazole and analyzed by Western blotting. (b) Immunocytochemical staining. Harvested cells were fixed and immunocytochemical stained with DAPI (blue), Cy3-labeled anti-SOD antibody (red), and FITC-MSN (green). HeLa cells were first pretreated with various concentrations of MSN-TAT-SOD, bare MSN, and TAT-SOD for 4 h. (c) The enzymatic assay of SOD. SOD specific activity was analyzed by pyrogallol method. (Details are in the Materials and Methods.)

cells and exhibit good cellular SOD activity. Results of the enzyme activity of SOD show an increase in a dose-dependent manner, which suggests that the denatured proteins were refolded to active form through chaperon assembly. We further examined whether the FMSN particles interfere with TAT-SOD in its activity. As compared to the activity of a positive control TAT-SOD (100 μg/mL), there is apparent similarity in activity when TAT-SOD formed the conjugates with FMSN matrix. Although there was no difference in SOD activity between FMSN-TAT-SOD and TAT-SOD, the MSN could serve as a multifunctional vehicle to load fluorescent organic dye, drugs, targeting peptides, and other biomoleculars such as siRNA. Evidently, these data confirm that the FMSN-TAT-SOD were efficiently delivered with full activity in HeLa cells. This is the first work reporting the MSN carrying denatured enzyme could refold in the cell with good activity. The MSN conjugated TAT-SOD was mediated by interactions of metal affinity. The Ni-NTA is extended from a tether with flexible arm. This avoids a large restriction from steric hindrance for modification, conformational change, and interactions of metal affinity. It also shows the delivered MSN as a multifunctional vehicle without interfering with the biological function of attached SOD molecules.

Previously, SOD has been reported with the biological functions of inhibiting cell apoptosis and ROS protection in mammalian cells.[36,37] Because FMSN-TAT-SOD has been successfully delivered and exhibits the antioxidant activity in HeLa cells, we then determined whether FMSN-TAT-SOD protects the cells from lipopolysaccharide (LPS) (50 μg/mL)-induced oxidative stress and paraquet-induced free radicals. First, we tested the effect of FMSN-TAT-SOD on cell viability of a MTT colorimetric assay under oxidative stress induced by LPS.[38] When pretreated with FMSN-TAT-SOD, the viability of LPS-treated cells was significantly increased in a dose-dependent manner. As shown in Figure 3a, when the cells

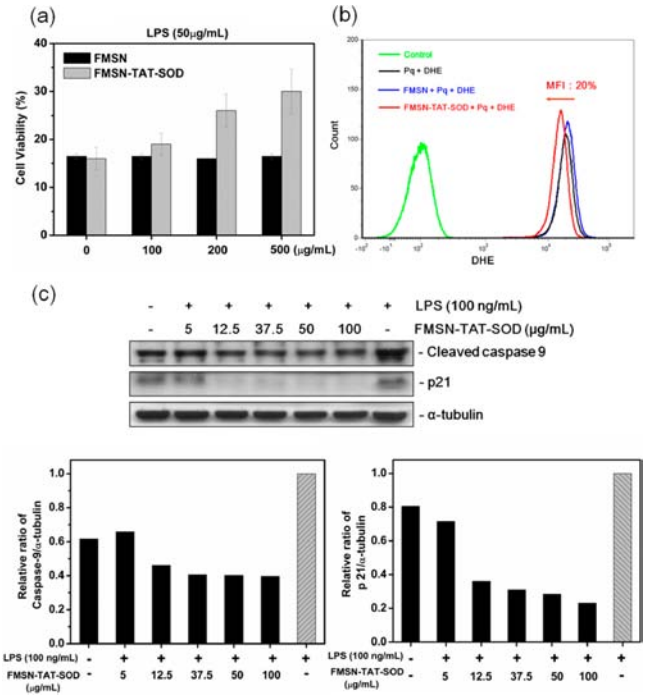

Figure 3. Inhibition of apoptosis, ROS protection, and activation of cleaved caspase-9 and p21 in HeLa cells by FMSN-TAT-SOD. HeLa cells were first pretreated with various concentrations of FMSN-TAT-SOD and control MSN for 4 h. (a) MTT assay. FMSN-TAT-SOD treated cells were exposed with LPS (50 μg/mL) for 18 h and determined the cell viability by a MTT colorimetric assay. (b) Detection of ROS generation. FMSN-TAT-SOD treated cells stimulated with paraquat (250 μM) and then oxidized dihydroethidine (DHE) dye (2 μM) were determined by flow cytometry analysis. (c) Western blotting analysis of cleaved caspase-9 and p21 protein. FMSN-TAT-SOD treated cells exposed to LPS (100 ng/mL) for 24 h, and the cellular levels of cleaved caspase-9 and p21 protein were analyzed by Western blotting. The quantitative data of Western blots were indicated by densitometric method.

were exposed to LPS with FMSN or without FMSN-TAT-SOD, only ~15% of cells stayed viable. However, the viability of the cells doubled when pretreated with FMSN-TAT-SOD at a high concentration. FMSN-TAT-SOD increases the cell viability from LPS-induced oxidative stress in a dose-dependent trend, suggesting that these fusion proteins on FMSN have a critical protective effect on cells against oxidative stress.

dx.doi.org/10.1021/ja3105208 | J. Am. Chem. Soc. 2013, 135, 1516−1523

To address the protective role of FMSN-TAT-SOD against the ROS-mediated apoptosis in HeLa cells, the cells were stimulated with paraquat (methyl viologen), which is well-known as an intracellular superoxide anion generator.[39,40] The amount of ROS was detected by reacting with dihydroethidine (DHE; Invitrogen)[41] and quantified by the red fluorescence detected in flow cytometric method. As shown in Figure 3b, the group with FMSN-TAT-SOD delivery (red) decreased 20% mean fluorescence values as compared to the control group with no additional treatment in paraquat stimulated cells (black), whereas FMSN delivered cells (blue) retain the same as the paraquet control. The nonparaquet stimulated cells (green) as a negative control have little oxidation of DHE. This suggested that the FMSN-TAT-SOD catalyze the superoxide dismutation to reduce the amount of free radicals. Thus, the risk of free radicals attacking the cells was reduced.

Most of the LPS-stimulated cell apoptosis involves activation of the cleaved caspase-9[42] and p21[43] protein signaling cascades mechanism. To examine the protective effect of FMSN-TAT-SOD on LPS-induced cleaved caspase-9 and p21 activation, cells were treated with the FMSN-TAT-SOD (5−100 μg/mL) for 4 h and subsequently exposed to LPS (100 ng/mL) for 24 h, and then the cellular cleaved caspase-9 and p21 was analyzed by Western blot analysis (Figure 3c). Western blotting results revealed that FMSN-TAT-SOD suppressed LPS-induced cleaved caspase-9 and p21 activation in a dose-dependent manner for HeLa cells. It indicates that FMSN-TAT-SOD was able to remove the free radicals (or reduces oxidative stress), which led to cell apoptosis in either caspase-9 signaling cascade or p21 activation.

Taken together, we have shown MSN is a good nanocarrier for the enzyme SOD. The MSN served as an inert carrier, which does not interfere much with normal biological function. From our experiments, we demonstrated FMSN-TAT-SOD still retains the antioxidant activities and protection of cell from apoptosis; ROS scavenger activity and p21 activation, which the native SOD performs, were illustrated.

As mentioned above, the full SOD activity of a denatured FMSN-TAT-SOD was restored through a refolding machinery. Because the Cu,Zn-SOD is a metalloenzyme containing copper and zinc ions, the molecular refolding to constitute the intact structure may also need the incorporation of metal ions, which is important for conformation and catalysis. In principle, through the supply of the essential metal ions, the metal-loenzymes would gain more activities if the ions are the limiting factor in the SOD activity in cells. With the addition of those metal ions, we examined whether the activity of FMSN-TAT-SOD would increase after the transduction in cell and molecular refolding. Copper ion (50 μM) and zinc ion (50 μM) were added into the HeLa cells culture and incubated for 24 h; FMSN-TAT-SOD and control FMSN were then added for 4 h, which is usually enough for performing the enzyme activity. The specific activity of SOD was determined by pyrogallol auto-oxidation method.[43] No significant enhancement of the activity was observed in those cells treated with additional metal ions in our experimental conditions. These results suggest that the metal ion for full activity of SOD may have been supplied by an endogenous source. Also in Figure 4a, results of an SOD specific kinetic analysis revealed that the SOD activity was markedly increased by the addition of FMSN-TAT-SOD as compared to the FMSN-only case. Also, it is moderately higher (40%) than the case of FMSN-SOD. That the FMSN-SOD still retains some minor activity indicated

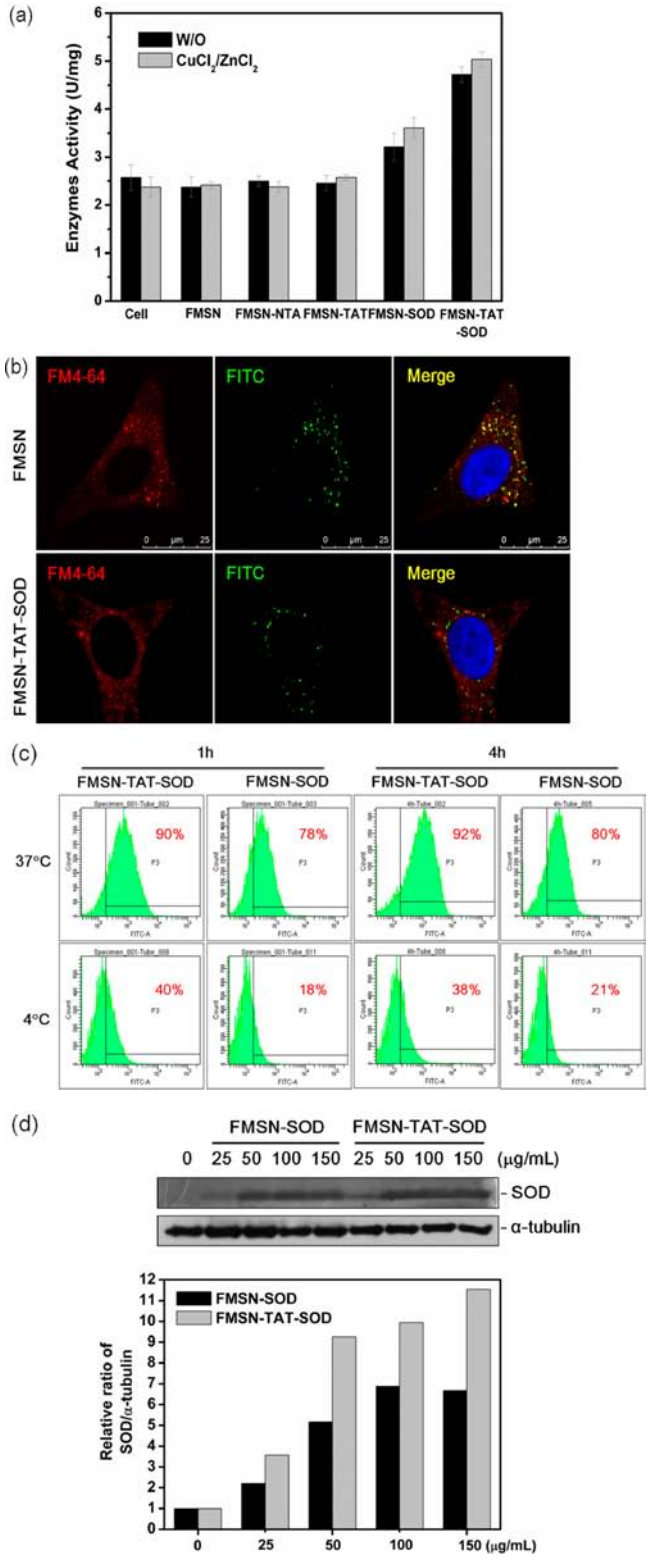

Figure 4. Effect of the TAT, Cu^{2+}, Zn^{2+}, and temperature on the delivery activity of SOD. HeLa cells were first pretreated with FMSN-TAT-SOD and control FMSN for 4 h. (a) Metal effect on the activity of FMSN-TAT-SOD. Copper ion (0.05 mM) and zinc ion (0.05 mM) were added into the culture medium and incubated for 24 h before FMSN-TAT-SOD and control FMSN treatment. The specific activity of SOD was determined by pyrogallol method. (b) Confocal microscopy analysis of MSN in endosome. The living unfixed cells were cotreated with endosome-specific marker FM 4−64 (5 μg/mL) and analyzed by confocal microscopy for an endosomal colocalization

dx.doi.org/10.1021/ja3105208 | J. Am. Chem. Soc. 2013, 135, 1516−1523

Figure 4. continued

image. The fluorescent images show the MSN (green, FITC) and FM 4−64-labeled endosomes (red). (c) Temperature effect on MSN endocytosis. The cells were incubated at 37 or 4 °C individually, and the cellular uptake of nanoparticles was determined by FACS analysis for cell endocytosis activity. (d) Delivery efficiency by Western blot analysis. Various concentrations of FMSN-TAT-SOD and FMSN-SOD were added into the cells, and the cellular level of SOD protein was measured in the cells by Western blotting.

some FMSN-SOD could perform nonendocytosis translocation without the TAT sequence.

While the cellular uptake of MSN has been shown to follow an endocytosis process,[22,23] the cellular uptake of the cationic TAT cell-penetrating peptide has been shown to follow a nonendocytosis mechanism.[44−46] In our experiment, we constructed a combinational FMSN-TAT cargo and successfully delivered the SOD protein into the HeLa cells. We then investigated possible mechanism for the uptake of the FMSN-TAT-SOD protein. FM4−64 dyes have been widely used to study endocytosis, vesicle trafficking, and organelle organization in living eukaryotic cells.[47] The FMSN or FMSN-TAT-SOD (green) was cocultured with FM4−64 (red) (Molecular Probes) to trace the distributions of certain specific molecule in living HeLa cells. As shown in the confocal microscopic results (Figure 4b), a punctate cytoplasmic distribution pattern for both FMSN and FMSN-TAT-SOD was observed. For the FMSN alone, the FMSN (green) predominantly co- localized with FM 4−64 (red, the marker of endosome) in living cells as indicated by the resulting yellow coloration, but the minority of green dots still remains. However, FMSN-TAT-SOD (green) shows a different distribution pattern from that of FM4−64, indicating they were not colocalized. These data suggest that the TAT peptide on FMSN-TAT-SOD allows the cargo delivery into cells through a nonendocytosis mechanism and avoids subsequent endosomal trapping, while FMSN alone would remain in endosomes. Many groups used chemically synthesized TAT peptides to conjugate on nanoparticles to reach the nonendocytosis mechanism approach. This work is the first to develop a protein expression system by molecular cloning method combined with nanoparticles for TAT-conjugation and delivery.

The efficiency of endocytosis is limited by the low lipid fluidity and available energy. Further evidence from cellular uptake at low temperature also illustrated some part of the FMSN-TAT-SOD delivery is an energy-independent process to drive a nonendocytosis translocation. The cellular uptake of FMSN-SOD and FMSN-TAT-SOD was measured by flow cytometry at 4 and 37 °C for 1 and 4 h. As shown in Figure 4c, the delivery efficiency of FMSN-TAT-SOD (90−92%) was better than FMSN-SOD (78−80%) at 37 °C for 1 and 4 h, which suggests that the TAT enhances the delivery more effectively. Experiments on both nanoparticles at 4 °C for 1 and 4 h showed a similar result (FMSN-TAT-SOD of 38−40% vs FMSN-SOD of 18−21%). However, the delivery efficiency was reduced at 4 °C because the low temperature decreased the endocytosis pathway. The 20% increase of uptake of FMSN-TAT-SOD as compared to FMSN-SOD at 4 °C indicates that the TAT provides a nonendocytosis delivery. Furthermore, our results from the cellular uptake experiment illustrated that the FMSN-TAT-SOD delivery at low temperature is still active. FMSN-TAT-SOD enhanced the uptake of cells through TAT-mediated nonendocytosis delivery at 4 °C as compared to FMSN-SOD.

TAT is the signaling peptide to help the delivery and avoid MSN-mediated SOD from the endocytosis. However, we found the FMSN-SOD without any TAT sequence still has some SOD activity. As shown in Figure 4a, FMSN-SOD had less activity as compared to FMSN-TAT-SOD. FMSN-SOD and FMSN alone would tanslocate through the endocytosis mechanism. Therefore, possibly most FMSN-SOD were trapped in endosomes, which resulted in loss of the activities. TAT played an important role for the nonendocytosis mechanism and enhanced the SOD activity significantly. We have demonstrated the TAT-SOD-mediated translocation is nonendosomal in contrast to FMSN alone. We further measured the amount of delivered FMSN-SOD and FMSN-TAT-SOD in cells, which may answer some of the questions about why FMSN-TAT-SOD retains high cellular activity. FMSN-SOD and FMSN-TAT-SOD were added to the serum free culture for 4 h. The relative quantities of delivered protein were then analyzed by Western blotting and densitometry. As shown in Figure 4d, high density of SOD band was determined in FMSN-TAT-SOD treated cells, indicating that FMSN-TAT-SOD was more efficiently delivered into cells than FMSN-SOD. The results support the FMSN carrying a TAT sequence will perform an efficient delivery of enzyme or other cargo, which has low endosomal trapping.

In conclusion, we have demonstrated that the MSN conjugated with TAT-SOD gave good dismutation activity toward superoxides in vitro. As a multifunctional vehicle, MSNs were modified by a Ni-NTA tether for interactions of metal affinity and by FITC for tracing the nanoparticle images. The conjugation of TAT mediates the nonendocytosis pathway, which MSN alone does not. To our best knowledge, this is the first report that the SOD conjugated on nanoparticles in denatured form was refolded after translocating in the cell. This success in protein delivery lays the groundwork for future complementation experiments and for eventual delivery of therapeutic proteins into patients in the form of protein treatment of ROS-mediated diseases.

METHODS

Materials and Methods. All chemicals were purchased from commercial suppliers (Acros, Aldrich, Sigma, and Merck) and were used without further purification.

Synthesis of Green Fluorescent Mesoporous Silica Nanoparticles. Following the literature method, C_{16}TABr (0.58 g, 1.64×10^{-3} mol) and 5 mL of 0.226 M ethanol solution of TEOS (1 mL of TEOS in 20 mL of 99.5% ethanol) were dissolved in 300 g of 0.51 M aqueous ammonia solution. The stock solution was stirred at 50 °C for 5 h. Five milliliters of 1.13 M ethanol solution of TEOS (5 mL of TEOS in 20 mL of 99.5% ethanol) and FITC-APTMS was added with vigorous stirring for 1 h and then aged statically at 50 °C for 24 h. FITC-APTMS, *N*-1-(3-trimethoxysilyl propyl)-*N*′-fluoreceyl thiourea), was prepared in advance by stirring fluorescein isothiocyanate (FITC, 1 mg) and 3-aminopropyltrimethoxysilane (APTMS, 5 μL) in 5 mL of ethanol (99%) at room temperature for 24 h. As-synthesized samples were then collected by centrifugation at 18 000 rpm for 10 min and washed five times with 99% ethanol. 200 mg of as-synthesized samples was redispersed in 25 mL of 95% ethanol with 0.5 g of 37 wt % HCl. Surfactant was extracted by heating the ethanol suspension at 60 °C for 24 h. The product, called FITC-MSN (FMSN), was collected by centrifugation, washed with ethanol several times, and stored in sterile water or ethanol.

Conjugation of NTA-Silane and Ni(II) with MSNs (FMSN-Ni-NTA). As-synthesized FMSN with template surfactants (50 mg)

dx.doi.org/10.1021/ja3105208 | *J. Am. Chem. Soc.* 2013, 135, 1516−1523

suspended in toluene (50 mL) containing NTA-silane (25 mg) were stirred under reflux for 18 h. The products were collected by centrifugation and washed with ethanol three times to eliminate unreacted silane. To remove the surfactants, the products were suspended in acidic ethanol (1 g of HCl in 50 mL of EtOH) and refluxed for 24 h. Subsequently, hydrolysis of methoxycarbonyl on NTA linker was achieved in the presence of aqueous ρ-TsOH (0.133 g, pH = 2) under stirring at 65 °C for 6 h. The products, called FMSN-NTA, were collected following the same procedure described above. Next, FMSN-NTA suspended in 50 mL of aqueous $NiCl_2$ (50 mM) was stirred at 25 °C for 6 h. Finally, the nickel coordinated FMSN-NTA (FMSN-Ni-NTA) was obtained after excess $NiCl_2$ was removed by ethanol washing.

Immobilization of His-TAT-SOD Proteins with FMSN-Ni-NTA. A crude cell lysate of *E. coli* containing His-TAT-SOD proteins was mixed and incubated with FMSN-Ni-NTA at 4 °C overnight. After that, the His-TAT-SOD conjugated with FMSN-Ni-NTA (FMSN-TAT-SOD) was isolated by centrifugation and washed several times with water as well as ethanol. Afterward, the FMSN-TAT-SOD was suspended and stored in ethanol at 4 °C.

Cell Lines and Reagents. The HeLa cell line was obtained from the American Type Culture Collection (Manassas, VA). Restriction endonucleases and T4 DNA ligase were purchased from Promega (Madison, WI). Oligonucleotides were synthesized from Gibco BRL (Gaithersburg, MD) customized primers. Isopropyl-L-D-thiogalacto-pyranoside (IPTG) was obtained from Promega. *Escherichia coli* strain JM109 (DE3) was obtained from Stratagene (La Jolla, CA). Human Cu,Zn-SOD cDNA fragment was isolated using the polymerase chain reaction (PCR) technique using the human liver cDNA library. Polyclonal antibodies raised against human Cu,Zn-SOD were produced in our laboratory.

Isolation of the Full-Length Human Cu,Zn-SOD. Total RNA was isolated from human liver using the RNAzol reagent (Tel-Test, Friendswood, TX) according to the instructions of the manufacturer. To isolate the cDNA covering the complete open reading frame (ORF) of human Cu,Zn-SOD according to the sequences of one human expressed sequence tag (accession number K00065, Genbank), the full-length human Cu,Zn-SOD was amplified with a Cu,Zn-SOD sense primer, CuZn-SOD-F, 5′-ATG GCG ACG AAG GCC GTG TGC GTG CTG-3′, and a Cu,Zn-SOD antisense primer, CuZn-SOD-R, 5′-TTA TTG GGC GAT CCC AAT TAC ACC ACA-3′. PCR amplification was performed in a 50 mL reaction mixture containing 2 mL of first-strand cDNA, 0.5 mg of primers, 1.5 mM $MgCl_2$, 0.2 mM dNTP, and 2.5 U of HiFi-DNA polymerase (Yeastern Biotech, Taipei, Taiwan). Samples were incubated in a thermal cycler (Hybaid MultiBlock System; Hybaid Limited, Franklin, MA). The cDNA from brain template was used for PCR amplification using the program of 94 °C for 3 min; 40 cycles of 94 °C for 30 s, 55 °C for 30 s, and 72 °C for 60 s; and a final extension step at 72 °C for 15 min. All products were ligated into pGEM-T easy vector (Promega) and subjected to sequence analysis.

Construction of Expression Clones. The expression plasmid pQE-SOD was constructed by inserting the full-length human Cu,Zn-SOD cDNA into pQE30 at the *Sph*I and *Pst*I sites, which allows generation of the Cu,Zn-SOD protein with in-framed His-tag at the N-terminal end. The pQE-TAT-SOD expression vector was constructed to express the basic domain (amino acids 49−57) of HIV-1 TAT as a fusion with Cu,Zn-SOD as follows. In brief, two oligonucleotides were synthesized and annealed to generate a double-stranded oligonucleotide encoding nine amino acids from the basic domain of HIV-1 TAT. Their sequences are (*Bam*HI-TAT-F) 5′-GAT CCG GAA GAA GCG GAG ACA GCG ACG AAG ACG-3′ and (*Bam*HI-TAT-R) 5′-GAT CCG TCT TCG TCG CTG TCT CCG CTT CTT CCG-3′. The double-stranded oligonucleotide was directly ligated into the *Bam*HI-digested pQE-SOD to generate the His-TAT-SOD expression plasmid pQE-TAT-SOD.

Expression and Purification of Recombinant Proteins. pQE-TAT-SOD was expressed in *E. coli* JM109. A colony of *E. coli* cells was separately inoculated into Luria−Bertani broth in the presence of 100 mg/mL ampicillin, and the culture was grown overnight at 37 °C until its optical density at 600 nm reached 1.2. To induce expression of these recombinant proteins, IPTG was added to a final concentration of 1.0 mM, and the incubation was continued for 1−3 h. All recombinant proteins were collected and purified with FMSN-Ni-NTA by metal affinity binding.

Cell Culture. HeLa cells, a human epithelial cervical cancer cell line, were maintained in Dulbecco's modified eagles medium supplemented (DMEM; GIBCO) with 10% fetal bovine serum (FBS; GIBCO), 100 U/mL penicillin, and 100 μg/mL streptomycin (GIBCO) at 37 °C in a humidified and 5% CO_2 atmosphere. When adherent cells reached ∼60−70% confluence, they were detached with 0.25% trypsin-EDTA growth medium to allow for continued passaging.

Western Blotting Analysis. Cell lysates were separated on a 10% SDS-PAGE, and the proteins were then electrophoretically transferred to a polyvinylidene difluoride (PVDF) membrane and blocked 1 h at toom temperature in blocking buffer [1xTris-buffered saline (TBS)−0.1% Tween 20, 5% w/v nonfat dry milk]. Membranes were incubated overnight at 4 °C with primary antibodies:cleaved-caspase 9 and p21 from Santa Cruz Biotechnology (Santa Cruz, CA), along with α-tubulin from Oncogene Science. All primary antibodies were diluted in dilution buffer [1xTris-buffered saline (TBS)−0.1% Tween 20, 5% w/v BSA]. The PVDF membranes were extensively washed and incubated with a horseradish peroxidase-conjugated goat anti-rabbit immunoglobulin G antibody (1:2000 dilution, Rockland, Inc.) for 1 h at room temperature. Immunoreactive bands were visualized with the enhanced chemiluminescence substrate kit (Amersham Pharmacia Biotech, GE Healthcare UK Ltd., Bucks, UK) according to the manufacturer's protocol.

Immunocytochemical Staining for TAT-SOD Expression. HeLa cells were fixed with 4% paprformaldehyde, and permeabilized with 0.1% Triton X-100. After being washed in PBS, cells were blocked with 3% skim milk for 1 h and then incubated with a polyclonal anti-human Cu,Zn-SOD antibody for 16 h at 4 °C. The cells were extensively washed and incubated with rabbit antihuman Cu,Zn-SOD antibody and visualized with antirabbit Cy^3-labeled secondary antibody at a 1/1000 dilution for 2 h, and counterstained for nuclei with DAPI (DNA marker) for 5 min. The fluorescent images were obtained on a confocal microscope (TCS SP5, Leica).

Determination of Superoxide Dismutase Activity. Superoxide dismutase (SOD) activity of cell lysates was measured according to the method of Marklund.[48] Superoxide anion radical is involved in the auto oxidation of pyrogallol. At alkaline pH, SOD dismutates superoxide, thereby inhibiting the auto-oxidation of pyrogallol. The stock pyrogallol solution contained 1.0 mL of 0.5 M HCl and was stored at 30 °C. The assay mixture, containing 500 μL of buffer (50 mM Tris−cacodylic acid buffer, pH 8.4, 1 mM diethylenetriamine pentaacetic acid, 1 mM potassium phosphate buffer, pH = 7.0), 50 μL of sample, and 400 μL of deionized water, was put into a cuvette. The control sample contained 500 μL of assay buffer and 450 μL of water. The optical density of each sample was measured at 420 nm before the addition of pyrogallol. The increase in absorbance was measured at 10 s intervals and lasted for 3 min. SOD specific activity was expressed as units per milligram (U/mg) of protein.

Cell Viability Assay. The 1×10^5 cells per well were seeded in 24-well plates for proliferation assays. After incubation with different amounts of nanoparticles suspended in serum-free medium for 4 h, respectively, then the lipopolysaccharide (LPS; 50 μg/mL; Sigma) was added to the culture medium for 18 h. Cell viability was estimated by a colormetric assay using MTT [3-(4,5-dimethylthiazol-2-yl)-2,5-diphenyl-tetrazolium bromide (0.5 mg/mL)]. The dark blue formazan dye generated by the live cells was proportional to the number of live cells, and the absorbance at 570 nm was measured using a microplate reader (Bio-Rad, model 680). Cell numbers were determined from a standard plot of known cell numbers versus the corresponding optical density.

Superoxide Detection. The production of superoxide anion was fluorometrically estimated using a fluorescent probe, dihydroethidine (DHE), which is oxidized to a fluorescent intercalator, ethidium, by cellular oxidants, in particular, superoxide radicals. To measure

superoxide anion generation, dihydroethidine (DHE; 2 μM; Invitrogen) was used. Increase in DHE fluorescence upon paraquat (superoxide anion generator) stimulation indicated an increase in superoxide anion levels. After various experimental treatments, cells were incubated with DHE for 20 min and trypsinized, followed by cytofluorimetric analysis with a FACS Calibur flow cytometry (BD Biosciences).

■ ASSOCIATED CONTENT

Supporting Information

Experimental methods for obtaining powder X-ray diffraction, nitrogen adsorption−desorption isotherms, TEM micrographs, flow cytometry analysis, and endosome staining and results in Figures S1−S5. This material is available free of charge via the Internet at http://pubs.acs.org.

■ AUTHOR INFORMATION

Corresponding Author

cymou@ntu.du.tw

Notes

The authors declare no competing financial interest.

■ ACKNOWLEDGMENTS

This work was supported by the National Science Council of Taiwan through the National Nanotechnology Program. We thank Mr. Si-Han Wu, Dr. Fan-Ching Chien, and Prof. Peilin Chen for technical help.

■ REFERENCES

(1) Vucic, S.; Kiernan, M. C. *Curr. Mol. Med.* **2009**, *9*, 255.
(2) Jeong, H. J.; Kim, D. W.; Woo, S. J.; Kim, H. R.; Kim, S. M.; Jo, H. S.; Park, M.; Kim, D. S.; Kwon, O. S.; Hwang, I. K.; Han, K. H.; Park, J.; Eum, W. S.; Choi, S. Y. *Mol. Cells* **2012**, *33*, 471.
(3) Feve, A. P. *CNS Neurol. Disord.: Drug Targets* **2012**, *11*, 450.
(4) Dube, K. N.; Bollini, S.; Smart, N.; Riley, P. R. *Curr. Pharm. Des.* **2012**, *18*, 799.
(5) Chung, E. J.; Lee, H. K.; Jung, S. A.; Lee, S. J.; Chee, H. Y.; Sohn, Y. H.; Lee, J. H. *Invest. Ophthalmol. Visual Sci.* **2012**, *53*, 379.
(6) Kashio, A.; Sakamoto, T.; Kakigi, A.; Suzuki, M.; Suzukawa, K.; Kondo, K.; Sato, Y.; Asoh, S.; Ohta, S.; Yamasoba, T. *Gene Ther.* **2012**, *19*, 1141.
(7) Kalkanidis, M.; Pietersz, G. A.; Xiang, S. D.; Mottram, P. L.; Crimeen-Irwin, B.; Ardipradja, K.; Plebanski, M. *Methods* **2006**, *40*, 20.
(8) Liu, L.; Guo, K.; Lu, J.; Venkatraman, S. S.; Luo, D.; Ng, K. C.; Ling, E. A.; Moochhala, S.; Yang, Y. Y. *Biomaterials* **2008**, *29*, 1509.
(9) Vallet-Regi, M. *Chem.-Eur. J.* **2006**, *12*, 5934.
(10) Slowing, I. I.; Trewyn, B. G.; Giri, S.; Lin, V. S. Y. *Adv. Funct. Mater.* **2007**, *17*, 1225.
(11) Sun, X. X.; Zhao, Y. N.; Lin, V. S. Y.; Slowing, I. I.; Trewyn, B. G. *J. Am. Chem. Soc.* **2011**, *133*, 18554.
(12) Mendez, J.; Monteagudo, A.; Griebenow, K. *Bioconjugate Chem.* **2012**, *23*, 698.
(13) Lin, Y. S.; Tsai, C. P.; Huang, H. Y.; Kuo, C. T.; Hung, Y.; Huang, D. M.; Chen, Y. C.; Mou, C. Y. *Chem. Mater.* **2005**, *17*, 4570.
(14) Li, C. *Catal. Rev.* **2004**, *46*, 419.
(15) Hoffmann, F.; Cornelius, M.; Morell, J.; Froba, M. *J. Nanosci. Nanotechnol.* **2006**, *6*, 265.
(16) Slowing, I. I.; Trewyn, B. G.; Lin, V. S. *J. Am. Chem. Soc.* **2007**, *129*, 8845.
(17) Radu, D. R.; Lai, C. Y.; Jeftinija, K.; Rowe, E. W.; Jeftinija, S.; Lin, V. S. Y. *J. Am. Chem. Soc.* **2004**, *126*, 13216.
(18) Torney, F.; Trewyn, B. G.; Lin, V. S. Y.; Wang, K. *Nat. Nanotechnol.* **2007**, *2*, 295.
(19) Lai, C. Y.; Trewyn, B. G.; Jeftinija, D. M.; Jeftinija, K.; Xu, S.; Jeftinija, S.; Lin, V. S. Y. *J. Am. Chem. Soc.* **2003**, *125*, 4451.
(20) Wu, S. H.; Hung, Y.; Mou, C. Y. *Chem. Commun.* **2011**, *47*, 9972.
(21) Li, Z. X.; Barnes, J. C.; Bosoy, A.; Stoddart, J. F.; Zink, J. I. *Chem. Soc. Rev.* **2012**, *41*, 2590.
(22) Huang, D. M.; Hung, Y.; Ko, B. S.; Hsu, S. C.; Chen, W. H.; Chien, C. L.; Tsai, C. P.; Kuo, C. T.; Kang, J. C.; Yang, C. S.; Mou, C. Y.; Chen, Y. C. *FASEB J.* **2005**, *19*, 2014.
(23) Chung, T. H.; Wu, S. H.; Yao, M.; Lu, C. W.; Lin, Y. S.; Hung, Y.; Mou, C. Y.; Chen, Y. C.; Huang, D. M. *Biomaterials* **2007**, *28*, 2959.
(24) Fridovich, I. *Annu. Rev. Biochem.* **1995**, *64*, 97.
(25) Lu, F.; Wu, S. H.; Hung, Y.; Mou, C. Y. *Small* **2009**, *5*, 1408.
(26) Chou, C. M.; Huang, C. J.; Shih, C. M.; Chen, Y. P.; Liu, T. P.; Chen, C. T. *Ann. N. Y. Acad. Sci.* **2005**, *1042*, 303.
(27) Coupland, P. G.; Briddon, S. J.; Aylott, J. W. *Integr. Biol.* **2009**, *1*, 318.
(28) Crowe, J.; Masone, B. S.; Ribbe, J. *Methods Mol. Biol.* **1996**, *58*, 491.
(29) Porath, J.; Carlsson, J.; Olsson, I.; Belfrage, G. *Nature* **1975**, *258*, 598.
(30) Guignet, E. G.; Hovius, R.; Vogel, H. *Nat. Biotechnol.* **2004**, *22*, 440.
(31) Howarth, M.; Takao, K.; Hayashi, Y.; Ting, A. Y. *Proc. Natl. Acad. Sci. U.S.A.* **2005**, *102*, 7583.
(32) Babu, P.; Sinha, S.; Surolia, A. *Bioconjugate Chem.* **2007**, *18*, 146.
(33) Lin, Y. C.; Liang, M. R.; Chen, C. T. *Chem.-Eur. J.* **2011**, *17*, 13059.
(34) Gottesman, S.; Wickner, S.; Maurizi, M. R. *Genes Dev.* **1997**, *11*, 815.
(35) Schneider, C.; SeppLorenzino, L.; Nimmesgern, E.; Ouerfelli, O.; Danishefsky, S.; Rosen, N.; Hartl, F. U. *Proc. Natl. Acad. Sci. U.S.A.* **1996**, *93*, 14536.
(36) Eum, W. S.; Choung, I. S.; Li, M. Z.; Kang, J. H.; Kim, D. W.; Park, J.; Kwon, H. Y.; Choi, S. Y. *Free Radical Biol. Med.* **2004**, *37*, 339.
(37) Lee, J. A.; Song, H. Y.; Ju, S. M.; Lee, S. J.; Kwon, H. J.; Eum, W. S.; Jang, S. H.; Choi, S. Y.; Park, J. S. *Exp. Mol. Med.* **2009**, *41*, 629.
(38) Messmer, U. K.; Briner, V. A.; Pfeilschifter, J. *Kidney Int.* **1999**, *55*, 2322.
(39) Yang, W. L.; Sun, A. Y. *Neurochem. Res.* **1998**, *23*, 47.
(40) Li, X.; Sun, A. Y. *J. Neural Transm.* **1999**, *106*, 1.
(41) Bindokas, V. P.; Jordan, J.; Lee, C. C.; Miller, R. J. *J. Neurosci.* **1996**, *16*, 1324.
(42) Chuang, C. Y.; Chen, T. L.; Cherng, Y. G.; Tai, Y. T.; Chen, T. G.; Chen, R. M. *Arch. Toxicol.* **2011**, *85*, 209.
(43) Tusell, J. M.; Saura, J.; Serratosa, J. *Glia* **2005**, *49*, 52.
(44) Frankel, A. D.; Pabo, C. O. *Cell* **1988**, *55*, 1189.
(45) Fawell, S.; Seery, J.; Daikh, Y.; Moore, C.; Chen, L. L.; Pepinsky, B.; Barsoum, J. *Proc. Natl. Acad. Sci. U.S.A.* **1994**, *91*, 664.
(46) Wadia, J. S.; Stan, R. V.; Dowdy, S. F. *Nat. Med.* **2004**, *10*, 310.
(47) Vida, T. A.; Emr, S. D. *J. Cell Biol.* **1995**, *128*, 779.
(48) Marklund, S.; Marklund, G. *Eur. J. Biochem.* **1974**, *47*, 469.